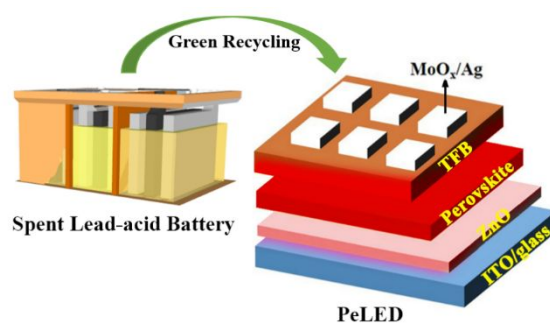


This document is confidential and is proprietary to the American Chemical Society and its authors. Do not copy or disclose without written permission. If you have received this item in error, notify the sender and delete all copies.

Recycling Spent Lead-acid Battery into Lead Halide for Resource Purification and Multifunctional Perovskite Diode

Journal:	<i>Environmental Science & Technology</i>
Manuscript ID	es-2021-01116g
Manuscript Type:	Article
Date Submitted by the Author:	16-Feb-2021
Complete List of Authors:	Li, Jiong; South China University of Technology Duan, Chenghao; South China University of Technology Yuan, Ligang; South China University of Technology Liu, Zidan; South China University of Technology Zhu, Hepeng; South China University of Technology Ren, Jianwei; University of Johannesburg, Department of Mechanical Engineering Science Yan, Keyou; South China University of Technology, School of Environment and Energy

SCHOLARONE™
Manuscripts

16 **TOC:**

17

18

19

20

21

22

23

24

25

26

27

28

29

30

31

32

33

34

35

36

37

38

39

40

41 **Abstract** Lead-acid battery is a reliable and cost-effective uninterrupted power supply
42 (UPS) for cars, wheelchairs and et al. Recycling the discarded lead-acid batteries has
43 increased the cost and could be a serious pollution issue after extensive use. It is
44 important to exploit the new-generation application to reduce the cost and increase the
45 value. In this article, we used a simple method to recycle spent lead-acid batteries for
46 useful lead iodide resource with a high purity of over 99% and a recycling yield of
47 91.6% and then fabricated multifunctional FAPbI₃ perovskite diode using recycled
48 lead iodide (PbI₂). The cost of recycled PbI₂ based on lab-grade chemicals is
49 estimated to be only 17.4% that of lab-grade PbI₂, which undoubtedly greatly reduces
50 the preparation cost of devices in the lab. The external quantum efficiencies (EQEs)
51 of our perovskite diodes prepared with commercial and recycled PbI₂ are 19.0% and
52 18.7%, respectively, which shows that the performance of the device prepared from
53 recycled PbI₂ is comparable to that of commercial lab-grade PbI₂. Based on the
54 expense of industrial-grade chemicals, the cost of recycled PbI₂ is extrapolated to be
55 77.8% that of industrial-grade PbI₂. In addition, the dosage for thin film electronics is
56 greatly diluted with respect to lead-acid batteries. Therefore, it can not only offer an
57 approach to recycle hazardous solid waste, but also save the manufacturing cost of
58 new-generation photoelectric devices, leading to earning additional value for lead
59 waste.

60

61 **Keywords:** Spent lead-acid batteries; Recycling; Lead halide; Perovskite diode; Low
62 cost.

63

64

65

66

67 INTRODUCTION

68 As a common energy storage device, lead-acid batteries are widely used in
69 automobiles, aviation, and navigation due to high discharge rate, durable
70 rechargeability, and low price^{1, 2}. In the discharge state of a lead-acid battery, the main
71 component of the positive electrode is lead dioxide and that of the negative electrode
72 is lead. In the charged state, the main component of the positive electrode and the
73 negative electrode is lead sulfate (PbSO₄). As more and more batteries die after
74 extensive usage, a lot of solid-state lead-acid wastes are produced to occupy plenty of
75 space. Particularly, the electrodes of lead-acid battery are mainly composed of Pb,
76 PbSO₄ and its oxides, which are easy to produce lead pollution. Recycling the lead
77 waster into battery will increase the additional cost. Aiming to start green
78 development, governments are promoting to standardize the lead-acid battery
79 industries and to recycle lead-acid batteries for advanced application^{3, 4}. Therefore,
80 how to recycle a large number of lead-acid batteries for utilization has become a new
81 scientific and engineering problem. Most of industries resort it to pyrometallurgical
82 process and wet chemistry for the recovery of the lead paste⁵⁻⁷. Because the
83 pyrometallurgical process often requires carbonaceous reducing agents, and produces
84 exhaust gases such as sulfur dioxide and carbon dioxide, which are seriously harmful
85 to the environment and the human health^{8, 9}. With the increasing requirements for
86 environmental protection, the hydrometallurgical recycling of spent lead-acid
87 batteries has displayed obvious advantages in this regard, but the existing
88 hydrometallurgical recycling process needs large waste water treatment capacity, high
89 energy consumption and complex production systems^{10, 11}. Therefore, there is an
90 urgent need for an economical and environmentally friendly way of recycling spent
91 lead-acid batteries to mitigate the pollution and earn additional value.

92 The traditional recycling process for lead-acid battery is well established for reuse
93 and the final lead product recovered is crude lead. The process is not so cost-efficient
94 that its own economic value is not very high^{12, 13}. Meanwhile, the industrially
95 recovered crude lead contains more impurities, which needs to be further purified for
96 advanced utilization. Halide lead perovskite materials have been widely used in the

97 research of solar cells and light-emitting diodes due to their abundant raw materials,
98 low cost, superior photoelectric properties, higher color purity, solution processing,
99 and low-temperature fabrication ($<150\text{ }^{\circ}\text{C}$)¹⁴⁻¹⁸. Just in ten years, the power
100 conversion efficiency (PCE) of perovskite solar cells (PSCs) has increased from the
101 initial 3.8% to the most recent 25.5%, and the electroluminescent external quantum
102 efficiencies (EQEs) of red and green light of perovskite light-emitting diodes
103 (PeLEDs) have also exceeded 20%, which receive worldwide research interest^{17, 19-23}.
104 At present, the lead element occupies a pivotal position in the most efficient PSCs and
105 PeLEDs, and thus the commercial lead source for lab use becomes more and more
106 expensive, which could also restrict the commercialization in the future. Therefore,
107 using lead resources from lead-acid batteries to fabricate the devices has two
108 advantages: (1) reasonably and properly mitigate the environmental problems caused
109 by spent lead-acid batteries, and realize the recycling of lead resources for advanced
110 application; (2) increase the additional value of the lead resource and reduce
111 manufacturing costs for advanced optoelectronic device. For example, PSC has
112 demonstrated to be highly stable in outer space application and thus could be widely
113 developed in low cost²⁴⁻²⁶. Therefore, it is feasible to recycle the lead source from
114 spent lead-acid batteries for perovskite materials and devices²⁷⁻³³.

115 In this work, we adopt the “wet-fire-wet” recycle process combining
116 pyrometallurgical and hydrometallurgical methods to recycle the spent lead-acid
117 batteries, which neither produces a mass of sulfur dioxide fumes that is harmful to the
118 environment like the pyrometallurgical method, nor does it produce a large amount of
119 waste water like the hydrometallurgical method. Firstly, we demonstrated the
120 preparation of lead iodide (PbI_2) powder from the lead source of lead-acid battery
121 through “wet-fire-wet” recycle process and the recycling yield is as high as 91.6%.
122 The extracted PbI_2 product is highly soluble in polar aprotic solvent but undissolved
123 in water and thus is facile for device utilization and environmental disposal. Then, the
124 as-prepared PbI_2 powder was used as the precursor solution to fabricate
125 high-brightness PeLEDs. The result shows that PbI_2 extracted by recycling lead in
126 spent lead-acid batteries has the same material characteristics as commercial PbI_2 , but

127 its cost is only 17.4% that of commercial lab-grade PbI_2 . By industrial scale-up, this is
128 extrapolated to be 77.8% that of industrial-grade PbI_2 . Therefore, we can develop
129 appropriate methods to recycle the waste lead sources for the fabrication of PeLEDs,
130 which not only saves the cost of device fabrication and earn additional value, but also
131 achieves the purpose of waste utilization and reduces environmental pollution.

132

133 **EXPERIMENTAL**

134 **Materials and Chemicals.** Ammonium carbonate ($(\text{NH}_4)_2\text{CO}_3$) (Cas no. 506-87-6,
135 purity: >99%), Hydrobromic acid (Cas no. 10035-10-6, ACS: 48%), $\text{Zn}(\text{Ac})_2 \cdot 2\text{H}_2\text{O}$
136 (Cas no. 557-34-6, purity: >98%), KOH (Cas no. 1310-58-3, purity: 99.99%) and
137 Hydroiodic acid (Cas no. 10034-85-2, ACS: 55-58%) were purchased from
138 Sigma-Aldrich. Nitric acid (Cas no. 7697-37-2, AR: 65-68%), Methanol (Cas no.
139 67-56-1, AR: 99.5%) and N, N-dimethylformamide (DMF) (Cas no. 68-12-2, purity:
140 >99%) were purchased from Aldrich. PbI_2 (Cas no. 10101-63-0, purity: 99.99%) and
141 Lead bromide (PbBr_2) (Cas no. 10031-22-8, purity: 99.99%) were purchased from
142 Xi'an Polymer Light Technology Corp.

143 **Extracting the lead resource for PbI_2 .** The spent lead-acid battery was obtained
144 from an abandoned electric bicycle. After removing the battery top cover, the battery
145 is mechanically disassembled. The acidic electrolyte was carefully poured out and
146 collected, and the inner wall of the battery and the electrode plate were repeatedly
147 washed with deionized water and dried. Scraped lead and its compounds from the
148 electrode plate were grinded into powder. The collected 21.6098 g powder scraped
149 from the electrode plate was firstly reacted with the slightly excessive ammonium
150 carbonate solution to desulfurize and placed overnight. After removing the
151 supernatant, the precipitate was collected. The precipitate obtained was dried in an
152 oven at 60 °C, and its main components are lead metal, lead dioxide, and lead
153 carbonate. The 19.04 g precipitate was calcinated in a tube furnace at 600 °C for 5
154 hours to obtain 15.4817 g yellow powder. The calcinated yellow powder (the main
155 component is PbO) was reacted with 2 mol/L dilute nitric acid diluted by 40 mL thick
156 nitric acid, stood for 2 hours, removed a small amount of impurity from the bottom.

157 The supernatant was reacted with 76 mL hydroiodic acid to obtain yellow PbI_2 crystal
158 powder, which was washed three times with ethanol, then recrystallized with DMF,
159 finally dried in a vacuum drying oven at 60 °C for 24 hours.

160 **Synthesis of ZnO NPs.** 2.95 g of $\text{Zn}(\text{Ac})_2 \cdot 2\text{H}_2\text{O}$ was dissolved in 125 mL of
161 methanol and 1.48 g of KOH was dissolved in 65 mL of methanol. $\text{Zn}(\text{Ac})_2 \cdot 2\text{H}_2\text{O}$
162 solution was added into a 250 mL three-neck round bottom flask and kept it to 60 °C,
163 and then KOH solution was poured to react for 2 hours. After keep overnight, the
164 supernatant was removed to collect the precipitate. After washing and centrifuging for
165 three times, it is finally dissolved in the mixed solution of methanol and chloroform
166 for use.

167 **Device fabrication.** The patterned ITO glass was washed with cleaning agent,
168 deionized water, acetone, isopropanol, absolute ethanol, and dried with nitrogen, and
169 then the substrate was further cleaned with UV-Ozone. In a fumehood, 8 mg/mL ZnO
170 as an electron transport material was spin-coated on the substrate at 4000 rpm for 60
171 s, and then annealed at 130 °C for 15 min. After cooling to room temperature, the
172 substrate was transferred to a nitrogen glove box for further device fabrication. FAI,
173 PbI_2 and 5AVA were dissolved in DMF at a molar ratio of 2: 1: 0.5 to prepare the
174 precursor solution with a concentration of 0.5 M. 30 μL of the perovskite precursor
175 solution was spin-coated on the substrate at 3000 rpm for 60 s, and TFB as the hole
176 transport material was spin-coated on the perovskite substrate at 2000 rpm for 30 s. 8
177 nm MoO_x and 100 nm Ag were sequentially deposited by vacuum evaporation
178 equipment (vacuum degree is 1.0×10^{-5} Pa), in which the effective area of the device
179 (the overlapping area of ITO and Ag electrodes) is 8 mm^2 .

180 **Characterization.** For PbO and PbI_2 powders, we use inductively coupled plasma
181 optical emission spectrometer (ICP-OES) (Model: CAP 7000) and ion chromatograph
182 (Model: ICS-1500) to conduct elemental composition analysis, and use X-ray
183 polycrystalline powder diffractometer (XRD) (Model: Empyrean) to verify the
184 material composition. For PbI_2 and precursor liquid films, we use XRD (Model:
185 Empyrean) for crystallinity analysis, and use ultra-high resolution field emission

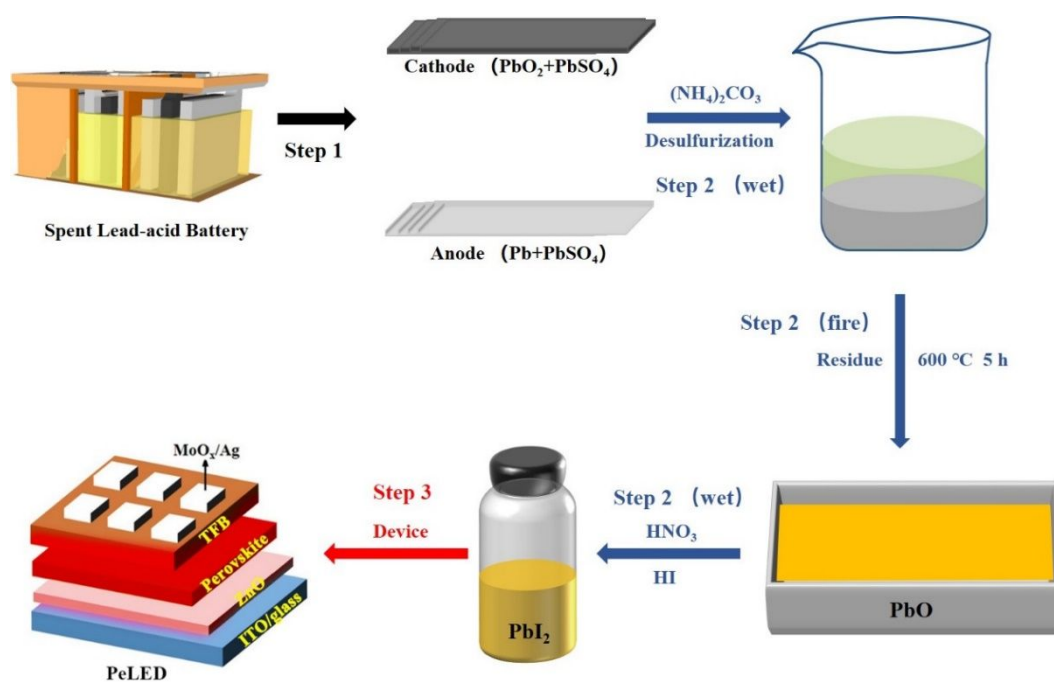
186 scanning electron microscope (SEM) (Model: Merlin) to characterize the surface
 187 morphology, using ultraviolet visible (UV) spectrophotometer (Model: UV-2600)
 188 measures its absorbance value. In addition, we used a 590 nm laser, an integrating
 189 sphere and a flame spectrometer to measure the photoluminescence quantum yield of
 190 the film.

191 We set up self-made test fixtures to test the electroluminescence performance of
 192 devices in an integrating sphere. Using Keithley 2400 instrument, at a step voltage of
 193 0.05 V, the J - V data from 0 V to 9 V is tested, and flame spectrometer (Ocean Optics)
 194 recorded electroluminescence characteristics.

195

196 Results and discussion

197



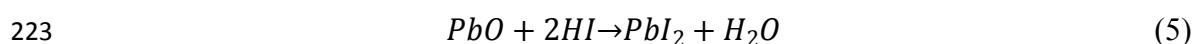
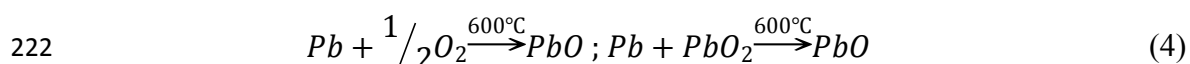
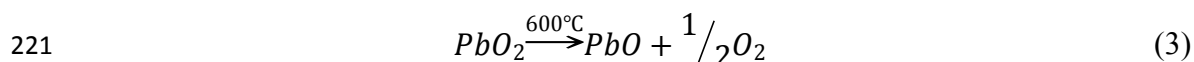
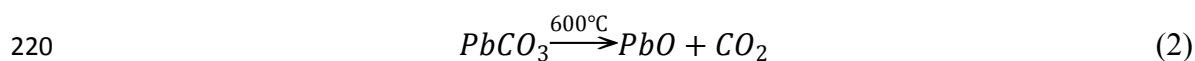
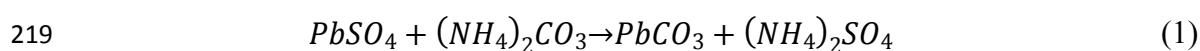
198

199 Figure 1. The recycling process of lead resource from spent lead-acid batteries for the fabrication
 200 of PeLED. Step 1: disassembly process; Step 2: “wet-fire-wet” recycling, including
 201 desulfurization, calcination and halide processes; Step 3: resource utilization for PeLED device.

202 Simple process, high yield and clean product are the grand goals for recycling the
 203 spent lead-acid battery. Figure 1 mainly shows the new recycling strategy for
 204 extracting high-purity PbI₂ powder by recycling spent lead-acid batteries and

205 fabricating high-brightness PeLEDs by using the recycled lead halide resource.
 206 Unlike traditional pyrometallurgical methods, this method not only contain no
 207 harmful flue gas (SO_x) and waste water, but also can extract high-purity lead halide
 208 powder with high productive yield due to the orthometric dissolution characteristic of
 209 lead halide (soluble in DMF but insoluble in water). This process is divided into three
 210 steps. Step 1 is the disassembly process, namely, removing the cathode and anode
 211 from the spent lead-acid battery. We took down the lead source electrode of the spent
 212 lead-acid battery and crushed it for standby. In Pb paste, it contains 50 wt% PbSO_4 ,
 213 28 wt% PbO_2 , 9 wt% PbO , 4 wt% Pb , and the total amount of Pb element is 70.76
 214 wt%. Step 2 is the “wet-fire-wet” recycle process for the high-purity PbI_2 , including
 215 wet-chemical desulphurization, fire calcination and wet-chemical halide through a
 216 series of chemical reactions. Step 3 is to utilize the extracted PbI_2 powder to prepare
 217 the perovskite precursor solution for fabricating PeLEDs.

218 In Step 2, the main chemical reactions are as follows:

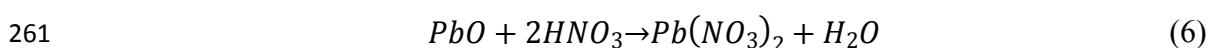


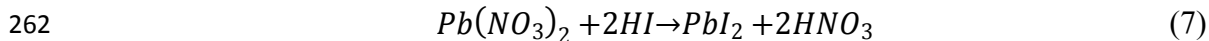
224 Due to the continuous charge-discharge cycle of lead-acid batteries, a large amount
 225 of PbSO_4 will be produced in both the anode and cathode, so when we process the
 226 electrode plate, we must first consider removing the sulfur element for subsequent
 227 treatment. In reaction (1), we add ammonium carbonate solution to the lead paste to
 228 make lead ions and carbonate ions produce insoluble precipitates, and then take the
 229 precipitates for later use to achieve the purpose of removing sulfur. The ICP test
 230 results of the reaction products show that the surface of the products may also be
 231 coated with a small amount of carbonate and ammonium ions and a very small
 232 amount of iron and antimony impurities (Sb: 0.01%; Fe: 0.1%), which may be caused

233 by the residual of unreacted ammonium carbonate in the precipitation process (Figure
234 S1). The ammonium sulfate produced is not only harmless to the environment, but
235 also can be used as a fertilizer for plants.

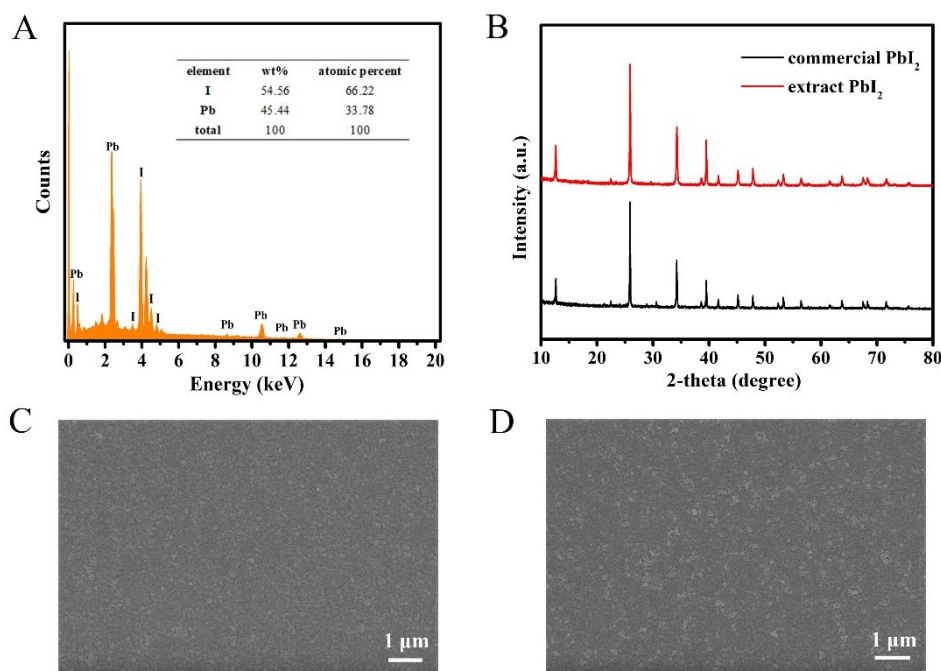
236 As shown in reaction (2-4), the lead carbonate, lead, and lead dioxide obtained by
237 the desulfurization reaction were calcinated in a tube furnace at 600 °C for 5 hours to
238 obtain yellow PbO powder without releasing harmful gas³⁴. In view of the new
239 pollution caused by the lead vapor generated by the oxidation of lead powder at 600
240 °C, the tail gas of lead powder was treated by using hydrogen iodide acid. On the one
241 hand, it can eliminate the environmental pollution caused by lead vapor. On the other
242 hand, the product of tail gas treatment and excess hydrogen iodide acid can be reused
243 to prepare PbI₂ without introducing impurities. Figure S2 shows the image of PbO
244 powder obtained by calcination. We further used various methods to characterize the
245 purity of PbO obtained by calcination. First, we used Scanning Electron
246 Microscope-Energy Dispersive Spectroscopy (SEM-EDS) to initially characterize the
247 purity of PbO. Through SEM, it can be seen that the PbO powder appears as large and
248 uniform crystals (Figure S3). As shown in Figure S4, the proportion of elements in the
249 PbO powder is analyzed by EDS. The proportion of lead element is 92.78%, the
250 proportion of oxygen element is 7.22%, and the atomic percentages of the two are
251 49.80% and 50.20%, which are close to 1: 1. It is preliminarily proved that the yellow
252 powder after calcination is PbO with a purity of about 100%. In addition, in order to
253 better verify the purity of PbO, the as-prepared PbO powder passed the ICP test
254 (Figure S5). The test results showed that the Pb content in the PbO powder reached
255 92.37%, and the purity exceeded 99.5%, reaching the purity of commercial PbO,
256 laying a good foundation for the next step to prepare high-purity lead halide.

257 Normally, we directly put the PbO powder beaker to react with hydroiodic acid
258 according to the stoichiometric ratio (reaction (5)). After a period of time, there is no
259 obvious change in the PbO powder. We speculate that PbI₂ is formed on the surface of
260 the PbO powder, which hinders the normal progress of the reaction.





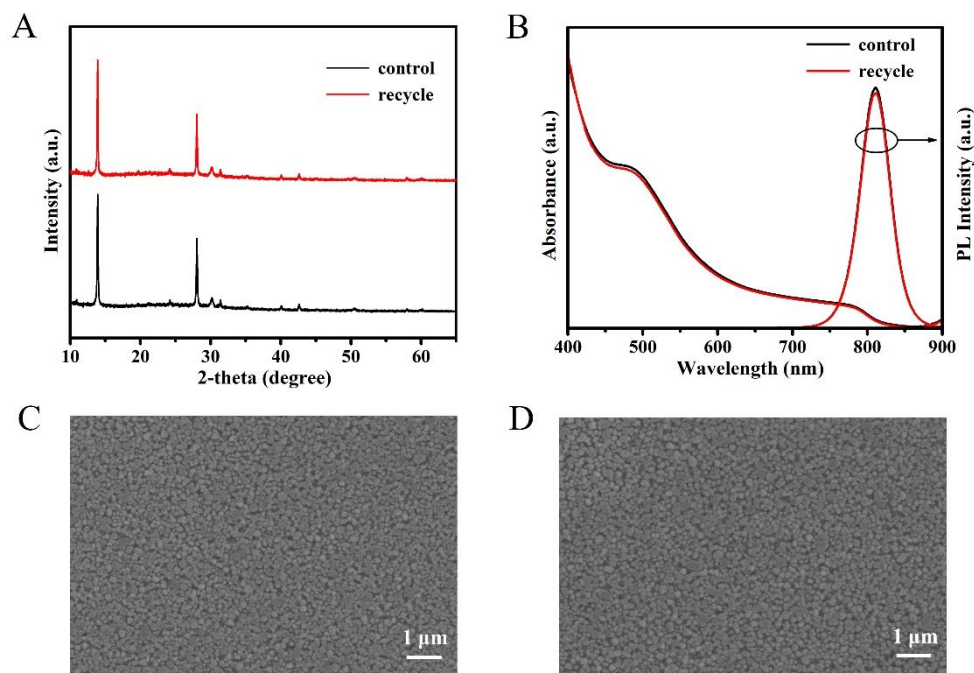
263 Therefore, we modified the process. The as-prepared PbO powder was first reacted
 264 with 2 mol/L of dilute nitric acid according to the stoichiometric ratio to obtain a clear
 265 solution, and there is no residue at the bottom of the beaker. 55-58 wt% HI was then
 266 added dropwise to the clear solution until yellow PbI₂ crystals no longer formed
 267 (reaction (6-7)). The HNO₃ generated by equation (7) can be reused to react with
 268 PbO.



269
 270 Figure 2. Material characterization for PbI₂ extracted from lead-acid batteries. (A) EDS analysis of
 271 PbI₂ powder. (B) XRD spectrum analysis of commercial and extracted PbI₂ powder. (C) SEM of
 272 the commercial PbI₂ film. (D) SEM of the extracted PbI₂ film.

273 The high purity of lead halide is the prerequisite for the preparation of performance
 274 PeLEDs. Further, since both antimony triiodide and ferrous iodide are soluble in
 275 ethanol and lead iodide is insoluble in ethanol, we washed PbI₂ powder with
 276 anhydrous ethanol for three times, and then recrystallized and purified with DMF to
 277 remove a small amount of iron and antimony impurities that may still exist. Finally,
 278 we dried in a vacuum oven at 60 °C for 24 hours to obtain pure yellow PbI₂ crystal
 279 powder (Figure S6). We performed the purity characterization of the extracted yellow
 280 PbI₂ crystal powder. We first performed EDS characterization of the extracted PbI₂

281 powder to determine its element content. As shown in the Figure 2A, the EDS
282 spectrum of extracted PbI_2 powder contains no other elements except Pb and I. The
283 mass fraction of I and Pb are 54.56% and 45.44%, respectively, so the purity of
284 extracted powder is close to 100%. The atomic percentages of I and Pb are 66.22%
285 and 33.78% by calculating, respectively, which are close to 2: 1. It is further confirms
286 that the molecular formula of the extracted white powder is PbI_2 . Figure 2B is the
287 XRD pattern of extracted PbI_2 from the spent lead-acid battery³⁵. It can be seen from
288 the XRD pattern that the extracted PbI_2 has the same crystal structure as the
289 commercial PbI_2 without redundant peaks and the intensity of the peaks varies
290 slightly, which indicates that the extracted PbI_2 with high purity will lay a foundation
291 for us to further prepare high-performance PeLED devices. The SEM images of PbI_2
292 powder shows that PbI_2 has a good cubic crystal structure, with a crystal size of about
293 500 nm (Figure S7). In order to verify the film-forming state of PbI_2 powder, we used
294 DMF as a solvent to prepare a 0.5 M PbI_2 solution and spin-coated it on a transparent
295 glass substrate. From Figure 2C, it can be seen that the SEM image of commercial
296 PbI_2 film exhibits good coverage without pinholes. Comparing the SEM images, we
297 can observe that the quality of extracted PbI_2 film is similar to that of commercial
298 PbI_2 film (Figure 2D). It is further verified that the extracted PbI_2 has good
299 film-forming ability, which is conducive to obtain high-quality perovskite films. We
300 also used an ultraviolet spectrophotometer to test the absorption spectra of the PbI_2
301 films, and the results showed that the commercial and extracted PbI_2 films have the
302 similar absorption spectrum (Figure S8).

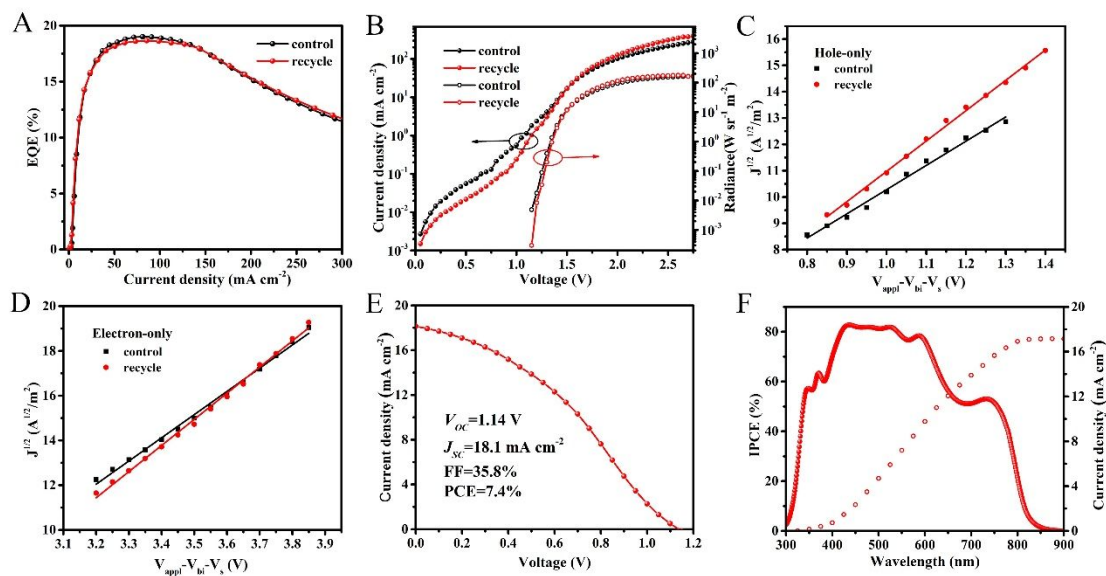


303

304 Figure 3. Film characterization of perovskite precursors. (A) XRD spectrum analysis of perovskite
 305 precursor. (B) The absorption peak and PL intensity of thin film of perovskite precursor. (C) SEM
 306 image of control perovskite precursor. (D) SEM image of recycle perovskite precursor.

307 We then used commercial and recycled PbI_2 as raw materials to prepare the FAPbI_3
 308 perovskite films. Through XRD analysis of the perovskite films prepared by
 309 commercial and extracted PbI_2 , we can see that two perovskite samples have good
 310 crystallinity and the same crystal structure (Figure 3A)³⁶⁻³⁸. It is well known that the
 311 optical properties of perovskite thin films affect the luminescence properties of
 312 PeLEDs. Therefore, it is necessary to study the absorption and fluorescence spectra of
 313 different FAPbI_3 perovskite films by UV-vis spectroscopy and photoluminescence
 314 (PL). Figure 3B shows the absorption spectra and PL spectra of the different
 315 perovskite films. It can be seen that two samples have a narrow PL peak at 809 nm
 316 and the absorption edge is also at 810 nm. We also studied the surface morphology of
 317 FAPbI_3 films prepared from different PbI_2 materials by SEM as shown in Figure 3C
 318 and D. Through SEM images, we can see that the perovskite film prepared from the
 319 extracted PbI_2 formed a uniform and dense thin film on the ZnO substrate, with a
 320 grain size of about 100 nm. The compact perovskite film with small size perovskite
 321 crystal is beneficial to increase the charge injection and reduce the non-radiative

322 recombination, so as to improve the electroluminescence performance of the device.
 323 Compared with the commercialized PbI_2 , the two samples have similar film states,
 324 which indicates that the PbI_2 extracted from the spent lead-acid battery will not affect
 325 the final efficiency of the device because of the quality of the light-emitting layer
 326 film, and can meet the preparation of perovskite film requirements.



327
 328 Figure 4. Device characterization of PeLEDs. (A) EQE diagrams of devices. (B) Current
 329 Density-Voltage-Radiance curves of devices. (C) $J^{1/2}$ - V_{app} - V_{bi} - V_s curves of hole-only devices. (D)
 330 $J^{1/2}$ - V_{app} - V_{bi} - V_s curves of electron-only devices. (E) J - V characteristic curves of corresponding
 331 device. (F) incident photon-to-electron conversion efficiency (IPCE) spectra of corresponding
 332 device.

333 In order to further evaluate the performance of the PeLEDs based on different
 334 sources of PbI_2 , we have fabricated the structure of PeLEDs with
 335 Glass/ITO/ZnO/FAPbI₃/TFB/MoO_x/Ag. As shown in Figure 4A, the commercial and
 336 extracted PbI_2 perovskite devices reached 19.0% and 18.7% peak EQE at a current
 337 density of 75 mA cm^{-2} , respectively, which further shows that the efficiency of the
 338 devices prepared by the recycled PbI_2 and commercial PbI_2 is almost the same. Figure
 339 4B shows the Current Density-Voltage-Radiance curves of the two devices from
 340 commercial and extracted PbI_2 . Due to the better carrier mobility of the device, when
 341 the bias voltage is applied to 1.2 V, the current density and radiance of the device
 342 prepared by the commercial PbI_2 increase rapidly, and the high brightness of 178 W

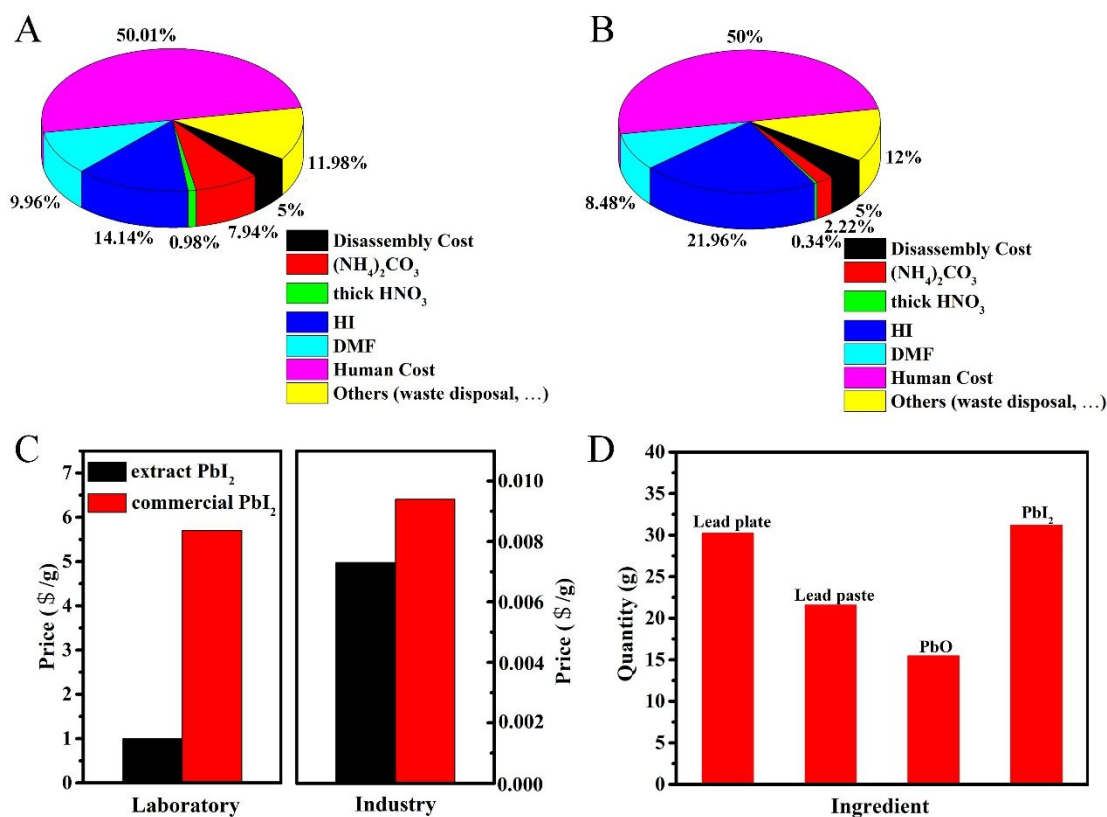
343 $\text{sr}^{-1} \text{m}^{-2}$ is reached at 2.6 V. Through comparison, it can be found that the maximum
344 brightness of the device prepared by the recycled PbI_2 is $173 \text{ W sr}^{-1} \text{m}^{-2}$ and the
345 brightness at the maximum EQE is $78 \text{ W sr}^{-1} \text{m}^{-2}$. In order to understand the
346 characteristics of PeLEDs based on different PbI_2 as raw materials, the hole and
347 electron mobilities of FAPbI₃ film (Figure 4C and D) were measured through the
348 space charge-limited current (SC-LC) model with a hole-only device of ITO/PEDOT:
349 PSS/FAPbI₃ (250 nm)/TFB/Ag structure and an electron-only device of
350 ITO/ZnO//FAPbI₃ (250 nm)/PC₆₁BM/Ag structure. Here the SC-LC is calculated by
351 the equation³⁹:

$$352 \quad J = \frac{9}{8} \epsilon_r \epsilon_0 \mu_e \frac{V^2}{d^3} \quad (8)$$

353 The results show that the hole mobility of FAPbI₃ films based on commercial and
354 extracted PbI_2 are 4.24×10^{-4} and $6.91 \times 10^{-4} \text{ cm}^2 \text{V}^{-1} \text{s}^{-1}$, and the electron mobilities of
355 them are 5.60×10^{-4} and $7.11 \times 10^{-4} \text{ cm}^2 \text{V}^{-1} \text{s}^{-1}$, respectively, which are of the same
356 order of magnitude and both have higher hole/electron mobility. A more matched
357 hole/electron mobility can improve the charge transport characteristics of the device,
358 thereby reducing nonradiative recombination and enhancing the performance of the
359 device. We also investigated the PV performance of PeLED. Figure 4E shows the J - V
360 curve of the corresponding LED device. We can observe that the device has a power
361 conversion efficiency (PCE) of 7.4% with a fill factor of 35.8%, an open circuit
362 voltage of 1.14 V, a short circuit current of 18.1 mA cm^{-2} . Figure 4F shows the IPCE
363 of the corresponding device, whose integral current is 17.2 mA cm^{-2} , which is
364 consistent with the current in the previous J - V curve.

365 In addition, we also use calcinated PbO to react with dilute nitric acid and
366 hydrobromic acid to prepare high-purity PbBr_2 (Figure S9). In order to verify the
367 purity of PbBr_2 , we performed EDS characterization on the PbBr_2 powder (Table S1).
368 The results showed that the white powder only contains Pb and Br, and the atomic
369 percentages of the two are 34.71% and 65.29%, respectively. The element ratio is
370 close to 2: 1. Further, we also compare the extracted PbBr_2 with commercial PbBr_2 ,
371 the XRD analysis showed that the two have the same crystal structure, and the

372 absorption spectrum further verified that the purity of the PbBr_2 we extracted is
 373 comparable to that of commercial PbBr_2 (Figure S10 and S11). In order to verify the
 374 optical properties of PbBr_2 , we used the extracted and commercial PbBr_2 to prepare
 375 CsPbBr_3 precursor to prepare PeLED of structure Glass/ITO/PEDOT: PSS/
 376 CsPbBr_3 /B3PyMPM/LiF/Al, in which the concentration of the active layer is 0.5 M.
 377 We also tested the electrical performance of the prepared devices, and the brightness
 378 of the commercial and extracted devices were 2288 and 2174 cd m^{-2} , respectively,
 379 indicating that the extracted PbBr_2 could achieve the photoelectric performance
 380 similar to that of the commercial PbBr_2 (Figure S12 and Video S1). We recovered
 381 lead from spent lead-acid batteries and extracted yellow PbI_2 and white PbBr_2
 382 powders to prepare high-performance PeLEDs. Through comparison, it is found that
 383 the PeLEDs prepared from the extracted perovskite raw materials and commercial
 384 raw materials have the same photoelectric properties, which provides a new idea for
 385 the recycling of used lead-acid batteries in the future.



386

387 Figure 5. Analysis on the benefits of lead recycling from spent lead-acid batteries. (A) Various

388 costs associated with the laboratory recycling process. (B) Various costs in the industrial recycling

389 process. (C) Comparison of recycling and commercial price of PbI_2 . (D) Yield analysis during
390 recycling.

391 In the manufacturing process of PeLEDs components, the main expense is the cost
392 of raw materials and human cost⁴⁰⁻⁴². By extracting PbI_2 from spent lead-acid
393 batteries, we not only save the manufacturing cost and increase the value, but also
394 make an important contribution to resource recovery and environmental pollution
395 reduction. We calculated the material consumption during the recycling process on
396 the basis of 100 g lead paste (Table 1). In the first disassembly process, the cost is set
397 to be 5% of the total budget. In the second step, the amount of ammonium carbonate,
398 thick nitric acid and hydroiodic acid are 0.033 kg, 0.04 L and 0.076 L, and the costs
399 are \$11.4, \$1.4 and \$20.3, respectively. DMF, used to purify PbI_2 multiple times,
400 costs about \$14.3, and other costs like waste disposal, pure water and lab equipment
401 costs are about \$17.2. It is worth noting that the human cost of extracting PbI_2 is set to
402 50% of the total cost, which is based on the budgeting of normal research project.
403 Finally, we calculated that the total cost of 100 g of paste for laboratory and industrial
404 recycling were \$143.6 and \$1.0555, respectively. As shown in Figure 5A and B, we
405 separately calculated the cost of each material in the whole battery in the laboratory
406 and the industrial recycling process. Compared with the laboratory recycling process,
407 the cost of $(\text{NH}_4)_2\text{CO}_3$ in the industrial recycling process is significantly reduced,
408 while the cost of HI is slightly increased. Meanwhile, DMF and nitric acid can be
409 reused in the extraction process of PbI_2 , so the actual recycling cost is even lower.
410 Further comparisons are made between the cost of recycled PbI_2 and the commercial
411 price of PbI_2 (Figure 5C). The price of known chemical reagent company's PbI_2 is 5.7
412 \$/g, while the laboratory recycling cost of our PbI_2 is 0.99 \$/g, which is only 17.4% of
413 the commercial cost. Even more surprising is that if we use industrial-grade raw
414 materials, the cost of extracting PbI_2 is only 77.8% that of industrial-grade PbI_2 ,
415 which greatly saves the preparation cost of PeLEDs.

416

417

418

419 **Table 1** The material consumption of 100 g lead paste.

Materials	Price		Dosage	Cost (\$)	
	Laboratory	Industry		Laboratory	Industry
(NH ₄) ₂ CO ₃	230 \$/kg	0.71 \$/kg	0.033 kg	11.4	0.0234
HNO ₃ (thick)	36 \$/L	0.09 \$/L	0.04 L	1.4	0.0036
HI	267 \$/L	3.05 \$/L	0.076 L	20.3	0.2318
DMSO	286 \$/L	1.79 \$/L	0.05 L	14.3	0.0895
Disassembly Cost				7.2	0.0528
Human Cost				71.8	0.5277
Others (Waste disposal ...)				17.2	0.1267
Total				143.6	1.0555

420 In the recycling process, the final recycling rate is an important indicator for our
 421 evaluation of the recycling of used lead-acid batteries. For this, we calculated the
 422 recycling rate by weighing the recycling amount at each step (Figure 5D). The lead
 423 paste of the spent lead battery is mainly the paste-like substance formed by the active
 424 material on the two poles after repeated charging and discharging. Its main
 425 components are PbSO₄, PbO₂, Pb, and the mass fraction of PbSO₄ exceeds 50%. We
 426 first take the active material off the electrode plate and obtain 21.6098 g powder. In
 427 step 2, we transfer the powder through desulfurization reaction and calcination
 428 reaction successively to obtain 15.4817 g of yellow PbO powder with a yield of about
 429 94%. The PbO powder is further reacted with dilute nitric acid and hydroiodic acid,
 430 and finally washing and vacuum drying, 31.1930 g of PbI₂ yellow crystal powder was
 431 obtained with a yield of about 97.5%. After calculation, the final yield was about
 432 91.6%.

433 **Table 2** Lead consumption of lead-acid battery and perovskite device.

		Dosage	Lead (each)	Lead (total)
		(million unit)	(kg)	(thousand tons)
lead-acid battery	electric moped	400	1	400
	car	1000	2	2000
perovskite device	display screen	5000	4.5×10 ⁻⁴	2.25

434 Reusing the lead source of spent lead-acid batteries for PeLEDs or perovskite
 435 display technology can not only reduce the economic cost of perovskite devices, but

436 also greatly reduce the environmental hazards because of the diluted concentration. A
437 preliminary evaluation of lead-acid batteries and perovskite display applications can
438 be made in terms of lead consumption and service life. From the perspective of
439 dosage, the application of lead-acid battery in the field of transportation is mainly to
440 provide power for electric moped and car. As shown in Table 2, there are about 400
441 million electric mopeds driven by lead-acid battery in the world, among which the
442 lead content of each lead-acid battery is calculated by 1 kg, which consumes a total of
443 400,000 tons of lead. What is even more surprising is that about 1 billion cars in the
444 world use lead-acid batteries as their uninterrupted power supply systems, and the
445 lead content of each uninterrupted power supply system is as high as 2 kg. So, just for
446 daily transportation, the amount of lead used is staggering 2.4 million tons. On the
447 other hand, the perovskite display screens mainly used for computer display in the
448 future, the size of each display screen is about 40 cm×50 cm, the thickness of the
449 perovskite active layer is 500 nm, and the concentration of lead in the perovskite film
450 is 4.5 g/cm³. If the number of laptops and PCs are 5 billion, the amount of lead used is
451 only 2,250 tons, which is only 0.1% of the amount of lead used in lead-acid batteries.
452 Therefore, if the lead source used in lead-acid batteries is recycled or directly used in
453 display technology, the amount of lead used will be greatly reduced, thereby reducing
454 the environmental problems caused by lead leakage. In terms of service life, the
455 longest service life of lead-acid batteries is 5 years, while the average life of display
456 screens is 8-10 years. Therefore, using recycled lead in perovskite display technology
457 is also a more low-carbon and environmentally friendly energy recycling method.

458 With the development of the economy, vehicles such as electric mopeds and cars
459 have gradually become the main means of transportation for people to travel.
460 However, lead-acid batteries, the scrap products of these vehicles, have become a
461 problem of environmental pollution to be solved. Therefore, recycling the lead in
462 spent lead-acid batteries has become an important research topic. The utilization of
463 lead resource for advanced devices may offer more opportunity to enhance the
464 additional value for hazardous wastes.

465 We use a combination of pyrometallurgical and hydrometallurgical methods to

466 recycle spent lead-acid batteries. Firstly, yellow PbO powder with purity more than
467 99.5% was obtained by treating spent lead-acid battery and calcinating at high
468 temperature. Then, the PbO powder was sequentially reacted with dilute nitric acid
469 and hydroiodic acid to obtain yellow PbI₂ crystals, washed with absolute ethanol for
470 multiple times, and recrystallized with DMF to obtain high-purity PbI₂ crystals with a
471 purity of more than 99% and a yield of 91.6%. This method of combining wet and fire
472 metallurgy methods to extract lead from spent lead-acid batteries can not only extract
473 high-purity perovskite raw materials, but also save energy consumption. Further, we
474 used extracted PbI₂ as raw materials to prepare the PeLEDs. Through the analysis of
475 the thin film and optical properties of the device, we found that the extracted PbI₂ has
476 the same physical and chemical properties as the commercial PbI₂, and the EQEs of
477 the devices prepared with extracted and commercial PbI₂ are 19.0% and 18.7%,
478 respectively, which shows that we can completely use the extraction of lead source
479 from the spent lead acid battery as the raw material for perovskite research. It not only
480 saves the cost problem, but also effectively reduces the environmental pollution
481 caused by the spent lead-acid batteries, leading to the lead source recycling and
482 utilization.

483

484 **ASSOCIATED CONTENT**

485 **Supporting Information**

486 Supporting Information is available free of charge on the ACS Publications website or
487 from the author.

488

489 **AUTHOR INFORMATION**

490 **Corresponding Author**

491 E-mail: kyyan@scut.edu.cn (K. Y.)

492 **Author Contributions**

493 # J. L. and C. D. contributed equally to this work.

494 **Notes**

495 Any additional relevant notes should be placed here.

496 **ACKNOWLEDGMENTS**

497 This work was in part supported by Start-up funds from Central Organization
498 Department and South China University of Technology, as well as fund from the
499 Guangdong Science and Technology Program (2020B121201003, 2019ZT08L075,
500 2019QN01L118).

501

502 **REFERENCES**

503 (1) Zhu, X.; Li, L.; Sun, X.; Yang, D.; Gao, L.; Liu, J.; Kumar, R. V.; Yang, J.,
504 Preparation of basic lead oxide from spent lead acid battery paste via chemical
505 conversion. *Hydromet.* **2012**, *117-118*, 24-31.

506 (2) Zeng, X.; Gong, R.; Chen, W. Q.; Li, J., Uncovering the Recycling Potential of
507 "New" WEEE in China. *Environ. Sci. Technol.* **2016**, *50*, (3), 1347-58.

508 (3) Goodenough, J. B.; Park, K. S., The Li-ion rechargeable battery: a perspective. *J.*
509 *Am. Chem. Soc.* **2013**, *135*, (4), 1167-76.

510 (4) Khor, A.; Leung, P.; Mohamed, M. R.; Flox, C.; Xu, Q.; An, L.; Wills, R. G. A.;
511 Morante, J. R.; Shah, A. A., Review of zinc-based hybrid flow batteries: From
512 fundamentals to applications. *Mater. Today Energy* **2018**, *8*, 80-108.

513 (5) Kreuzsch, M. A.; Ponte, M. J. J. S.; Ponte, H. A.; Kaminari, N. M. S.; Marino, C.
514 E. B.; Mymrin, V., Technological improvements in automotive battery recycling.
515 *Resour. Conserv. Recy.* **2007**, *52*, (2), 368-380.

516 (6) Lyakov, N. K.; Atanasova, D. A.; Vassilev, V. S.; Haralampiev, G. A.,
517 Desulphurization of damped battery paste by sodium carbonate and sodium
518 hydroxide. *J. Power Sources* **2007**, *171*, (2), 960-965.

519 (7) Yu, W.; Zhang, P.; Yang, J.; Li, M.; Hu, Y.; Liang, S.; Wang, J.; Li, S.; Xiao, K.;
520 Hou, H.; Hu, J.; Kumar, R. V., A low-emission strategy to recover lead compound
521 products directly from spent lead-acid battery paste: Key issue of impurities removal.
522 *J. Clean. Prod.* **2019**, *210*, 1534-1544.

- 523 (8) Santos, S. M.; Neto, J. C.; Silva, M. M., Forecasting model to assess the potential
524 of secondary lead production from lead acid battery scrap. *Environ. Sci. Pollut. R.*
525 **2019**, *26*, (6), 5782-5793.
- 526 (9) Yu, W.; Zhang, P.; Yang, J.; Li, M.; Hu, Y.; Liang, S.; Wang, J.; Li, S.; Xiao, K.;
527 Hou, H., A low-emission strategy to recover lead compound products directly from
528 spent lead-acid battery paste: Key issue of impurities removal. *J. Clean. Prod.* **2019**,
529 *210*, 1534-1544.
- 530 (10) Liu, W.-f.; Deng, X.-b.; Zhang, D.-c.; Yang, T.-z.; Chen, L., A clean process of
531 lead recovery from spent lead paste based on hydrothermal reduction. *Tran.*
532 *Nonferrous Met. Soc. China* **2018**, *28*, (11), 2360-2367.
- 533 (11) Ma, Y.; Qiu, K., Recovery of lead from lead paste in spent lead acid battery by
534 hydrometallurgical desulfurization and vacuum thermal reduction. *Waste Manag.*
535 **2015**, *40*, 151-6.
- 536 (12) Zhu, X.; He, X.; Yang, J.; Gao, L.; Liu, J.; Yang, D.; Sun, X.; Zhang, W.; Wang,
537 Q.; Kumar, R. V., Leaching of spent lead acid battery paste components by sodium
538 citrate and acetic acid. *J. Hazard. Mater.* **2013**, *250-251*, 387-96.
- 539 (13) Machado Santos, S.; Cabral Neto, J.; Mendonca Silva, M., Forecasting model to
540 assess the potential of secondary lead production from lead acid battery scrap.
541 *Environ. Sci. Pollut. Res. Int.* **2019**, *26*, (6), 5782-5793.
- 542 (14) Quan, L. N.; García de Arquer, F. P.; Sabatini, R. P.; Sargent, E. H., Perovskites
543 for Light Emission. *Adv. Mater.* **2018**, *30*, (45), 1801996.
- 544 (15) Kim, Y. H.; Kim, J. S.; Lee, T. W., Strategies to Improve Luminescence
545 Efficiency of Metal-Halide Perovskites and Light-Emitting Diodes. *Adv. Mater.* **2018**,
546 *31*, (47), 1804595.
- 547 (16) Dunlap-Shohl, W. A.; Zhou, Y.; Padture, N. P.; Mitzi, D. B., Synthetic
548 Approaches for Halide Perovskite Thin Films. *Chem. Rev.* **2018**, *119*, (5), 3193-3295.
- 549 (17) Cao, Y.; Wang, N.; Tian, H.; Guo, J.; Wei, Y.; Chen, H.; Miao, Y.; Zou, W.; Pan,
550 K.; He, Y.; Cao, H.; Ke, Y.; Xu, M.; Wang, Y.; Yang, M.; Du, K.; Fu, Z.; Kong, D.;
551 Dai, D.; Jin, Y.; Li, G.; Li, H.; Peng, Q.; Wang, J.; Huang, W., Perovskite
552 light-emitting diodes based on spontaneously formed submicrometre-scale structures.

- 553 *Nature* **2018**, *562*, (7726), 249-253.
- 554 (18) Wang, J.; Song, C.; He, Z.; Mai, C.; Xie, G.; Mu, L.; Cun, Y.; Li, J.; Wang, J.;
555 Peng, J.; Cao, Y., All-Solution-Processed Pure Formamidinium-Based Perovskite
556 Light-Emitting Diodes. *Adv. Mater.* **2018**, *30*, (39), 1804137.
- 557 (19) Dong, Y.; Zhao, Y.; Zhang, S.; Dai, Y.; Liu, L.; Li, Y.; Chen, Q., Recent
558 advances toward practical use of halide perovskite nanocrystals. *J. Mater. Chem. A*
559 **2018**, *6*, (44), 21729-21746.
- 560 (20) Cao, X.; Zhi, L.; Jia, Y.; Li, Y.; Zhao, K.; Cui, X.; Ci, L.; Zhuang, D.; Wei, J., A
561 Review of the Role of Solvents in Formation of High-Quality Solution-Processed
562 Perovskite Films. *ACS Appl. Mater. Interfaces* **2019**, *11*, (8), 7639-7654.
- 563 (21) Lin, K.; Xing, J.; Quan, L. N.; de Arquer, F. P. G.; Gong, X.; Lu, J.; Xie, L.;
564 Zhao, W.; Zhang, D.; Yan, C.; Li, W.; Liu, X.; Lu, Y.; Kirman, J.; Sargent, E. H.;
565 Xiong, Q.; Wei, Z., Perovskite light-emitting diodes with external quantum efficiency
566 exceeding 20 per cent. *Nature* **2018**, *562*, (7726), 245-248.
- 567 (22) Akihiro Kojima, K. T., ‡ Yasuo Shirai,§ and Tsutomu Miyasaka, Organometal
568 Halide Perovskites as Visible-Light Sensitizers for Photovoltaic Cells. *J. Am. Chem.*
569 *Soc.* **2009**, *131*, 6050–6051.
- 570 (23) Best Research-Cell Efficiencies. <https://www.nrel.gov/pv/cell-efficiency.html>
- 571 (24) Tang, Z.; Uchida, S.; Bessho, T.; Kinoshita, T.; Wang, H.; Awai, F.; Jono, R.;
572 Maitani, M. M.; Nakazaki, J.; Kubo, T., Modulations of various alkali metal cations
573 on organometal halide perovskites and their influence on photovoltaic performance.
574 *Nano Energy* **2018**, *45*, 184-192.
- 575 (25) Li, C.; Guo, Q.; Zhang, H.; Bai, Y.; Wang, F.; Liu, L.; Hayat, T.; Alsaedi, A.;
576 Tan, Z., Enhancing the crystallinity of HC(NH₂)₂PbI₃ film by incorporating
577 methylammonium halide intermediate for efficient and stable perovskite solar cells.
578 *Nano Energy* **2017**, *40*, 248-257.
- 579 (26) Reb, L. K.; Bohmer, M.; Predeschly, B.; Grott, S.; Weindl, C. L.; Ivandekic, G. I.; Guo, R.
580 J.; Dreißigacker, C.; Gernhäuser, R.; Meyer, A.; Buschbaum, P. M.; Perovskite and Organic
581 Solar Cells on a Rocket Flight. *Joule* **2020**, *4*, 1880-1892.
- 582 (27) Dhiaputra, I.; Permana, B.; Maulana, Y.; Inayat, Y. D.; Purba, Y. R.; Bahtiar,

- 583 A., Composition and crystal structure of perovskite films attained from electrodes of
584 used car battery. *AIP Conference Proceedings* **2016**, 1712, 050013.
- 585 (28) Chen, P.-Y.; Qi, J.; Klug, M. T.; Dang, X.; Hammond, P. T.; Belcher, A. M.,
586 Environmentally responsible fabrication of efficient perovskite solar cells from
587 recycled car batteries. *Energy Environ. Sci.* **2014**, 7, (11), 3659-3665.
- 588 (29) Li, C.; Zhu, Z.; Wang, Y.; Guo, Q.; Wang, C.; Zhong, P.; Tan, Z. a.; Yang, R.,
589 Lead acetate produced from lead-acid battery for efficient perovskite solar cells. *Nano*
590 *Energy* **2020**, 69, 104380.
- 591 (30) Sun, X.; Yang, J.; Zhang, W.; Zhu, X.; Hu, Y.; Yang, D.; Yuan, X.; Yu, W.;
592 Dong, J.; Wang, H.; Li, L.; Vasant Kumar, R.; Liang, S., Lead acetate trihydrate
593 precursor route to synthesize novel ultrafine lead oxide from spent lead acid battery
594 pastes. *J. Power Sources* **2014**, 269, 565-576.
- 595 (31) Chen, L.-C.; Tien, C.-H.; Ou, S.-L.; Lee, K.-Y.; Tian, J.; Tseng, Z.-L.; Chen,
596 H.-T.; Kuo, H.-C.; Sun, A.-C., Perovskite CsPbBr₃ Quantum Dots Prepared Using
597 Discarded Lead-Acid Battery Recycled Waste. *Energies* **2019**, 12, (6), 1117.
- 598 (32) Kadro, J. M.; Pellet, N.; Giordano, F.; Ulianov, A.; Müntener, O.; Maier, J.;
599 Grätzel, M.; Hagfeldt, A., Proof-of-concept for facile perovskite solar cell recycling.
600 *Energy Environ. Sci.* **2016**, 9, (10), 3172-3179.
- 601 (33) Binek, A.; Petrus, M. L.; Huber, N.; Bristow, H.; Hu, Y.; Bein, T.; Docampo, P.,
602 Recycling Perovskite Solar Cells To Avoid Lead Waste. *ACS Appl. Mater. Interfaces*
603 **2016**, 8, (20), 12881-12886.
- 604 (34) Liu, T.; Qiu, K., Removing antimony from waste lead storage batteries alloy by
605 vacuum displacement reaction technology. *J. Hazard. Mater.* **2018**, 347, 334-340.
- 606 (35) Sharma, N.; Ashraf, I. M.; Khan, M. T.; Shkir, M.; Hamdy, M. S.; Singh, A.;
607 Almohammed, A.; Ahmed, F. B. M.; Yahia, I. S.; AlFaify, S., Enhancement in
608 photodetection properties of PbI₂ with graphene oxide doping for visible-light
609 photodetectors. *Sensors and Actuators A: Physical* **2020**, 314, 112223.
- 610 (36) Gwisu Kim* H. M.; Kyoung Su Lee; Do Yoon Lee; So Me Yoon; Sang II
611 Seok†, Impact of strain relaxation on performance of a-formamidinium lead iodide
612 perovskite solar cells. *Science* **2020**, 370, 108–112.

- 613 (37) Akin, S.; Akman, E.; Sonmezoglu, S., FAPbI₃-Based Perovskite Solar Cells
614 Employing Hexyl-Based Ionic Liquid with an Efficiency Over 20% and Excellent
615 Long-Term Stability. *Adv. Funct. Mater.* **2020**, *30*, (28), 2002964.
- 616 (38) Yang, S.; Liu, W.; Zuo, L.; Zhang, X.; Ye, T.; Chen, J.; Li, C.-Z.; Wu, G.; Chen,
617 H., Thiocyanate assisted performance enhancement of formamidinium based planar
618 perovskite solar cells through a single one-step solution process. *J. Mater. Chem. A*
619 **2016**, *4*, (24), 9430-9436.
- 620 (39) Duan, C.; Liu, Z.; Yuan, L.; Zhu, H.; Luo, H.; Yan, K., PEDOT: PSS-Metal
621 Oxide Composite Electrode with Regulated Wettability and Work Function for
622 High-Performance Inverted Perovskite Solar Cells. *Adv. Optical Mater.* **2020**, *8*, (17),
623 2000216.
- 624 (40) Chen Z.; Fang G.; Li H.; Zheng X.; G. F., Low-Cost Carbazole-Based
625 Hole-Transport Material for Highly Efficient Perovskite Solar Cells. *ChemSusChem*.
626 **2017**, *10*, 3111–3117.
- 627 (41) Yang, F.; Liu, J.; Lu, Z.; Dai, P.; Nakamura, T.; Wang, S.; Chen, L.; Wakamiya,
628 A.; Matsuda, K., Recycled Utilization of a Nanoporous Au Electrode for Reduced
629 Fabrication Cost of Perovskite Solar Cells. *Adv. Sci.* **2020**, *7*, (6), 1902474.
- 630 (42) Sajid, S.; Elseman, A. M.; Wei, D.; Ji, J.; Dou, S.; Huang, H.; Cui, P.; Li, M.,
631 NiO@carbon spheres: A promising composite electrode for scalable fabrication of
632 planar perovskite solar cells at low cost. *Nano Energy* **2019**, *55*, 470-476.
- 633